*Bangladesh Journal of Physics, Vol. **31**, Issue 2, pp. 75 – 81, December 2024*

A COMPARATIVE STUDY ON SURFACE MORPHOLOGY, OPTICAL AND THERMAL BEHAVIOUR OF UNDOPED AND Cu DOPED ZnO NANOSTRUCTURES

PARVIN SULTANA[1] , RAHIMA NASRIN [2,*], I. Z. ZEBIN[3], TULI HALDER[3], S. M. T. ISLAM[3] AND MOHAMMAD JELLUR RAHMAN[1]

[1]Department of Physics, Bangladesh University of Engineering and Technology, Dhaka-1000, Bangladesh
[2]Department of Physics, University of Barisal, Barisal-8200, Bangladesh
[3]Department of Physics, Government Brojomohun College, Barisal, National University, Gazipur, Bangladesh

**Corresponding author e-mail: muktanasrin77@gmail.com, **1st and 2nd authors have equal contribution*
Received on 12.12.2023, Revised received on 15.08.2024, Accepted for publication on 15.08.2024

DOI: *https://doi.org/10.3329/bjphy.v31i2.79521*

ABSTRACT

The undoped and Cu doped ZnO (Cu:ZnO) nanostructures were successfully synthesized by the chemical bath deposition (CBD) technique to study the influence of copper (Cu) content on its surface morphology, elemental, optical and thermal properties. Powder X-ray diffraction (XRD), Field Emission Scanning electron microscopy (FESEM), energy dispersive X-ray spectroscopy (EDX), ultraviolet-visible (UV-vis) spectroscopy, Thermogravimetric analysis (TGA) and differential scanning calorimetry (DSC) techniques have been used for different characterization. XRD studies showed hexagonal wurtzite ZnO nanostructures, The FESEM analysis revealed that the shape of the undoped ZnO were flower-like structures and the addition of Cu content influenced the morphology of the samples The flower-like structures were changed into a mixed structure with 6 wt% Cu concentration. Interestingly, the flower-like nanostructures were reproduced with smaller grain sizes for 9 wt% Cu content. The EDX results confirmed the presence of Zinc (Zn) and Oxygen (O)and Copper (Cu). In the UV–visible study, the highest band gap energy is obtained for undoped ZnO. The estimated band gap energy was found within the range of (2.95-1.48) eV. The DSC spectra of undoped ZnO displayed an endothermic peak around 211 ℃ whereas a representative 6 wt% Cu Doped ZnO displayed two endothermic peaks around 147 ℃ and 199 ℃.

Keywords: *ZnO nanostructure, X-ray diffraction, chemical bath deposition, surface morphology*

1. INTRODUCTION

Zinc oxide (ZnO) is regarded as one of the most important semiconductor oxide materials because of its size dependent unique properties and potential applications in fields such as gas sensors, solar cells, photocatalysts, etc. [1-4]. ZnO is an n-type semiconductor material having a wide direct band gap energy of 3.37 eV, a large exciton binding energy of 60meV at room temperature and it is thermally and chemically stable, less toxic, easy growth at low cost. The properties of ZnO strongly depend on their nanostructures. ZnO in the nano regime possesses different morphologies (particles, rods, sponges, flowers, etc.) that have a significant impact on their properties. The properties of ZnO can also be tuned by doping with various transition metals like Mn, Fe, Co, Ni, and Cu [5-10]. Among different transition metals, we have chosen Cu as a dopant [11] because it has a similar ionic radius as that of ZnO and it has high electrical conductivity. Moreover, the incorporation of Cu^{2+} ions yields different nanostructures. Nanocrystalline ZnO with various

morphologies has been effectively prepared by different methods such as microwave-assisted synthesis, hydrothermal synthesis, sol-gel synthesis, chemical bath (CBD), thermal decomposition, and electrochemical synthesis [12-14]. A large no of research works on transitional metal doped ZnO nanostructures has been reported**.** Yang et al. [15] synthesized Co-doped ZnO nanoparticles (CZO) via a novel freeze-drying route. Ahmad et al. [16] investigated the microstructure, optical and magnetic properties of Mn doped ZnO NPs synthesized by a solid-state reaction route. Sajjad et al. [13] prepared undoped and Cu-doped ZnO NPs using the chemical co-precipitation method. Cu doping has significantly enhanced visible PL which is possibly important for photo-catalyst and solar cell devices. Koao et al. [14] studied the surface morphology, structural and optical behaviour of undoped and Eu doped ZnO NPs. The scanning electron microscope (SEM) images depicted the flower-like shape of undoped and hexagonal-shaped Eu-doped ZnO NPs samples. In this research work, undoped and Cu: ZnO nanostructures with different concentrations of Cu content were prepared through the CBD method, followed by structural, thermal, morphological and optical characterization. This method is advantageous over other methods because it does not require high temperature and pressure and is suitable for large-scale deposition.

2. EXPERIMENTAL DETAILS

2.1 Sample preparation procedure

All the chemicals used for the preparation of the ZnO nanostructures were analytical grade. It includes zinc acetate [Zn $(CH_3COO)_2.2H_2O$)], copper acetate [$Cu(CH_3COO)_2.2H_2O$], thiourea [$(NH_2)_2CS$] and ammonia (25% NH_3). Ammonia was used as a complexing agent. For the preparation of undoped ZnO, 0.45 M of zinc acetate and 0.18 M of thiourea were dissolved in 80 ml of deionized water separately. Then, 19 ml of ammonia was added to 80 ml of deionized water. The chemical bath solution was prepared as follows: 60 ml of zinc acetate, thiourea and ammonia solutions were mixed in the constant ratio of 1:1:1. The mixture was continuously stirred for 20 min. After that, the solution was heated to 80°C and kept for a few min while continuously stirring. The resulting precipitates were left overnight and separated from the solvent by titration. The prepared ZnO was washed with acetone, ethanol and deionized water for the removal of any unreacted precursors. Then, the obtained precipitates were dried at ambient conditions for 72 h. For the synthesis of Cu: ZnO, different amounts of $Cu(CH_3COO)_2.2H_2O$ were added to obtain (3, 6, 9) wt % concentration of Cu.

2.2 Characterization Techniques

The crystal structure of the samples was determined with a Bruker D8 advanced Model diffractometer with Cukα (1 .541 8Å) radiation. The surface morphological characterization of the prepared NPs was performed by FESEM [JEOL-JSM 7600F, Japan]. The accelerating voltage was kept at 20 kV. The stoichiometric ratio of prepared undoped ZnO and Cu doped ZnO NPs were determined by EDX analysis. The analysis of the optical behaviours of samples was carried out in the wavelength range between 200 to 800 nm using a Perkin Elmer UV/Vis Lambda 20 spectrophotometer. Differential scanning calorimetry (DSC) analysis of all samples was conducted under a nitrogen atmosphere (20 ml min^{-1}) using a Perkin Elmer Pyris-1 differential scanning calorimeter (Waltham, Massachusetts, U.S.A). For DSC measurements 5-10 mg sample was used. The sample was heated from 30º to 600°C at the rate of 10 °C/ min.

3. RESULTS AND DISCUSSION

3.1 XRD analysis

The phase composition and crystallite structure of the synthesized samples were determined with the aid of powder X-ray diffraction. The diffraction pattern revealed that the synthesized ZnO and Cu: ZnO nanostructures are polycrystalline in nature as shown in Fig. 1. All the diffraction peaks can be indexed to the hexagonal wurtzite crystal structure of ZnO. The diffraction peaks of undoped ZnO with (100), (002), (101), (102), (110), (103), (200) and (112) are consistent with standard ZnO JCPDS Card. No. 89-7102. Two additional peaks were marked as (◆) was attributed to the Zn $(OH)_2$ according to the available powder diffraction JCPDS data of 38-0356. Terek et al. observed the same behaviour of Zn $(OH)_2$ for the as-synthesized ZnO nanostructures [15]. In 6 wt% Cu doped ZnO, there were other crystal phases of CuO marked as (*), $Cu(OH)_2$ marked as (Δ) and Cu_2O (•) along with ZnO. These may be attributed to the low solubility. The crystal planes and 2θ values of CuO are in close agreement with JCPDS Card No. 89-5898.

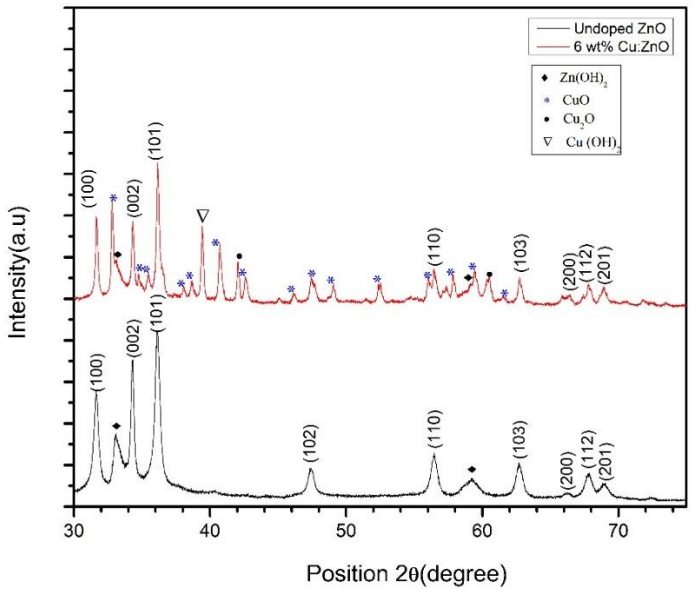

Fig. 1. X-ray powder diffraction patterns for undoped and 6 wt% Cu-doped ZnO prepared by CBD method.

3.2 Surface Morphology Analysis

Fig.2 displayed the FESEM micrographs of the undoped and a representative 6% Cu-doped ZnO NPs sample. The SEM images was taken at ×10K field of view. It is exhibited that the FESEM image of undoped ZnO NPs are flower-like structures, which composed of cones. With increasing the amount of Cu dopant, the density of particles increases and flower-like structures become completely altered with clustered irregular mixed structure with slight other material attached to the main structures. Sajjad et al.[13] synthesized undoped and Cu-doped ZnO NPs via chemical co-precipitation method where undoped ZnO NPs are not composed of flower-like structure but they are granular shape agglomerated as observed by SEM. As Cu content is increased to 7 Wt% the particle seems to be more agglomerated shape. This discrepancy may be due to different deposition/synthesis technique.

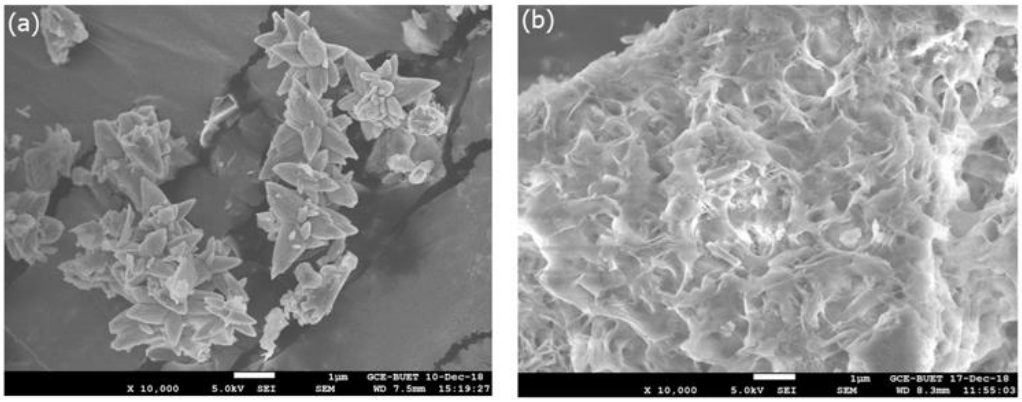

Fig. 2.SEM micrographs of (a) undoped ZnO and (b) a representative 6% Cu-doped ZnO.

3.3 Elemental analysis

The energy dispersive spectra (EDS) of undoped ZnO and 6% Cu: ZnO are exhibited in Fig. 3 (a) and (b) respectively. The spectra confirmed the presence of Zn and O elements in the undoped ZnO sample, while Cu, Zn and O elements were present in the 6% Cu: ZnO samples. Fig. 3 (b) confirmed the Cu incorporation in the host lattice.

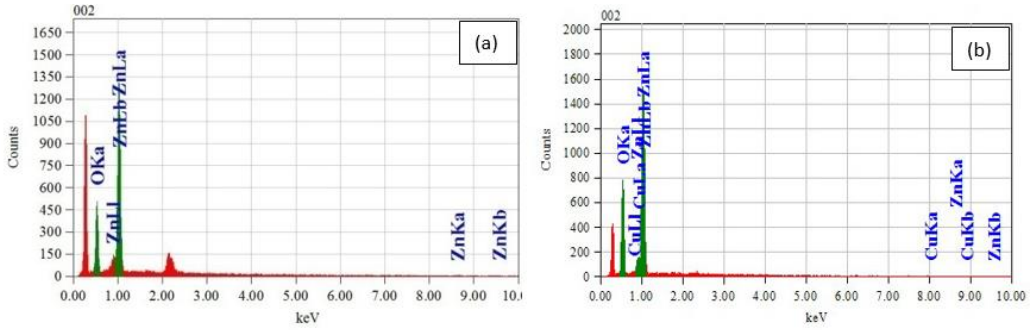

Fig. 3. EDS spectra of ZnO nanostructures for (a) undoped ZnO (b) 6 wt% Cu: ZnO.

3.4 Optical properties

The ZnO is a direct bandgap material. Diffuse reflectance spectral studies in the UV-Vis-NIR region were carried out to determine the optical bandgap E_g of the samples. The energy bandgap was estimated using the Kubelka-Munk function, $K = (1 - R)^2/2R$ for direct transitions [19]. The estimated band gap energy for 6 wt% and 9 wt% of Cu: ZnO were 2.03 eV and 1.48 eV, respectively. This reduction of E_g may be due to the surface defects density of undoped ZnO [20]. Another observation is that the E_g value exhibits decreasing trends upon the increase of Cu concentration, which agrees very well with the previous report [13]. The estimated value of E_g, determined from the curves of Figure 4 is documented in Table 2.

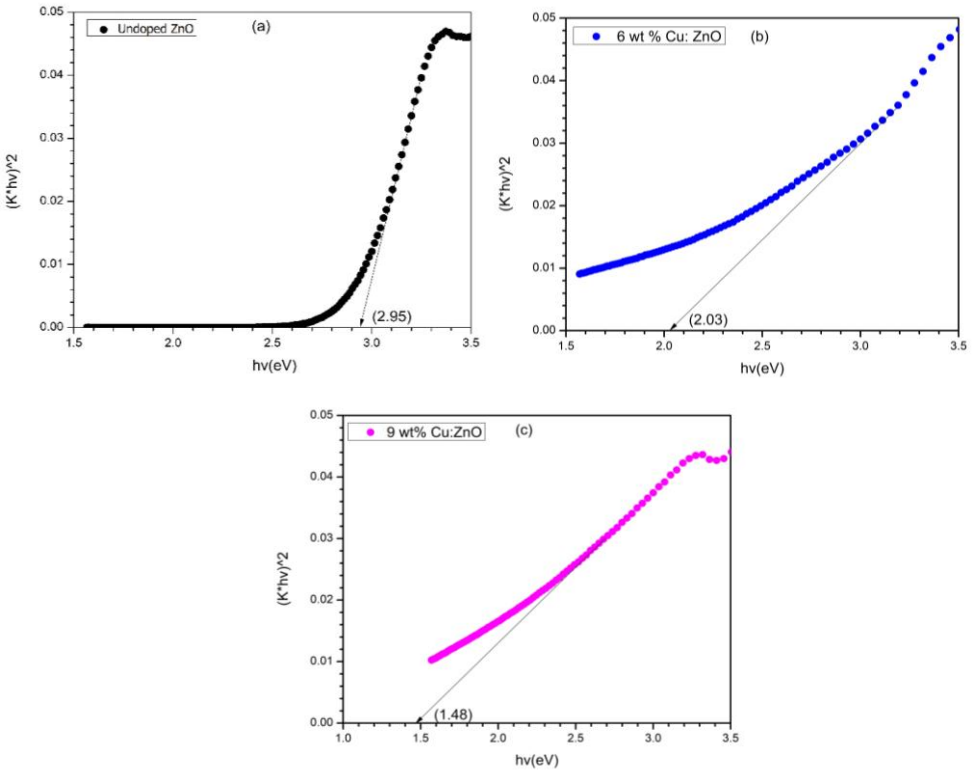

Fig. 4. Determination of the band gap energy of (a) undoped ZnO, (b) 6 wt% and (c) 9 wt% Cu: ZnO nanostructures.

Table 1: Optical bandgap of the undoped and Cu: ZnO nanostructures deposited at different doping concentrations.

Composition	**Band gap**
Undoped ZnO	2.95eV
6 wt% Cu: ZnO	2.03 eV
9 wt% Cu: ZnO	1.48eV

3.5 Thermal Properties

Thermo-gravimetric analysis (TGA)/differential scanning calorimetry (DSC) analysis is carried out to study the decomposition and phase formation that occurs while heating. The thermal heating is performed in the temperature range of 0-600°C with an increment of 10 °C /min. The TGA/DSC spectra of the undoped ZnO are presented in Fig. 5 (A). It is observed that the thermal decomposition took place in three steps. The initial weight loss from room temperature up to 110 °C is due to the evaporation of the water content [21]. The second weight loss between 110 and 212 °C might be ascribed to the decomposition of chemically bound groups with an endothermic

peak at 212 °C. The last weight loss from 280 to 420 °C might be due to the volatilization and combustion of organic species. Further, in the temperature range between 430 to 600 °C, no weight loss is detected. This indicated the formation of well crystalline ZnO as the decomposition product. On the other hand, the TGA/DSC spectra of 6 wt% Cu: ZnO nanostructures are presented in Fig. 5 (B). The DSC spectra of 6 wt% Cu: ZnO displayed two endothermic peaks around 147 °C and 199 °C respectively. This is due to the change of phases at that temperature.

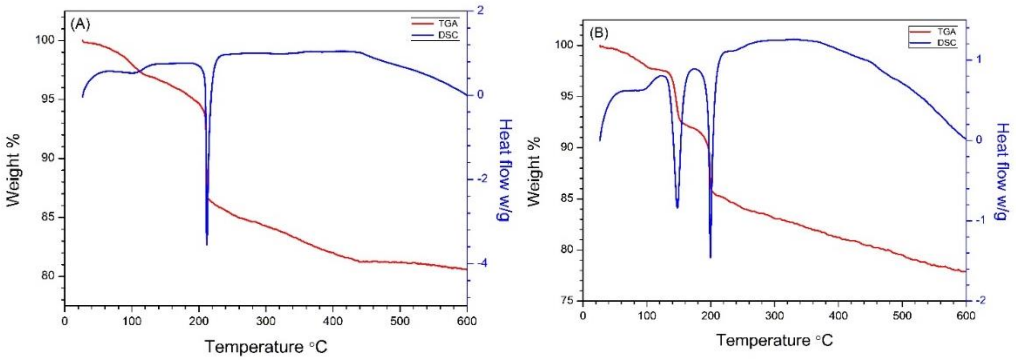

Fig. 5. The TGA/DSC spectra of (A) undoped and (B) 6 wt% Cu: ZnO nanostructures.

4. CONCLUSIONS

In this research, undoped ZnO and Cu: ZnO nanostructures have been successfully synthesized using a simple and economical CBD method varying the concentration of Cu content at a bath temperature of 80 °C. The SEM images depicted the formation of flower-like structures for undoped ZnO. After 6 wt% Cu doping, the flower-like structure became clustered and changed to a flakes-like shape. The flower-like structure with a smaller grain was reappeared when 9 wt% Cu impurity added. EDX results confirmed the presence of Zn, O and Cu contents. The UV-visible spectroscopy results showed that the bandgap energy is highest for the undoped flower-like ZnO nanostructures and gradually decreased with the increase of Cu content. The thermal study showed the stability of the undoped and Cu: ZnO The DSC spectra displayed endothermic peaks. Thus, it can be concluded that semiconducting oxide undoped ZnO and Cu: ZnO nanostructures may be used for application in optoelectronic devices.

ACKNOWLEDGEMENTS

The authors are thankful to the Department of Physics, BUET for permitting the lab facilities and Department of Nanomaterials and Ceramic Engineering, BUET and Bangladesh Council of Scientific & Industrial Research (BCSIR) for the characterization used for this study.

AUTHORS' STATEMENT

Parvin Sultana: Reviewing and Editing, Joint Supervisor, Rahima Nasrin: Reviewing and Editing, Supervisior, I. Z. Zebin: Writing- Original draft preparation Methodology, Investigation, Tuli halder: Investigation, Data curation, S. M. T. Islam: Joint supervisor, Mohammad Jellur Rahman: Reviewing and Editing, Joint Supervisor

REFERENCES

[1] N. J. Dayan, S. R. Sainkar, R. N. Karekar and R. C.Aiyer, Thin Solid Films, **325**, (1998) 254.
[2] R. Brayner, S.A Dahoumane, C. Yéprémian, C. Djediat, M. Meyer, A. Couté and F. Fiévet, Langmuir, **26**, (2010) 6522.
[3] C.W. Bunn Proc. Phys. Soc. London, **47**, (1935) 835.
[4] A. Hernandezbattez, R. Gonzalez, J. Viesca, J. Fernandez, J. Diazfernandez, A. MacHado, R. Chou and J. Riba, Wear **265**, (2008) 3.
[5] K. Yuan, X. Yin, J. Li, J. Wu, Y. Wang, F. Huang, J. Alloys Compd. **489** (2010) 694.
[6] L. Vayssieres, K. Keis, S.E. Lindquist and A. Hagfeldt, J. Phys. Chem. B. **105**, (2001) 3350.
[7] Y. Bakha, K.M. Bendimerad and S. Hamzaoui, Eur. Phys. J. Appl. Phys. **55**, (2011) 30103.
[8] L.R. Bekkaria, D. laânaba, R. Boyerb, B. Mahioub, C. Jaber Mater. Sci. Semicond. Process. **71**, (2017) 181.
[9] N. Saito, H. Haneda, T. Sekiguchi, N. Ohashi, L. Sakaguchi and K. Koumoto, Adv.Mater., 14, (2002) 418.
[10] K. L. Chopra, and S. R. Das, Thin Film Solar Cells (New York: Plenum) **9** (1983) 321.
[11] M.Sajjadi, I. Ullahd, M.I. Khanb, Jamshid Khaw, M. Yaqoob Khana, M. T. Qureshi' Results in Physics **9**, (2018) 1301.
[12] S. Hussain, T. Liu, M. Kashif, L. Lin, S. Wu, W. Guo, W. Zeng, U. Hashim, Material Science in Semiconductor Processing, 18 (2014) 52-58.
[13] H. Liu, J. Yang, Z. Hua, Y. Zhang, L. Yang, L. Xiao, Z. Xie, Appl. Surf. Sci. 256 (2010) 4162.
[14] L.F. Koao1, B.F. Dejene, H.C. Swart and T.E. Motaung, Int. J. Luminescence and Apllication. **5** (2015) 54-61.
[15] H. Yang and S. Nie, Materials Chemistry and Physics, **114**, (2009) 279.
[16] S.A. Ahmed, Results in Physics **7**, (2017) 604.
[17] L.F. Koao, B.F. Dejene, H.C. Swart, Optical Mater. **60** (2016) 294. Physica B, 439 (2014)173–176.
[18] T.T. Ali, K. Narasimharao, LP. Parkin, C. J. Carmalt, S. Sathasivam, S. N. Basahel, S. M. Bawaked, S. A. Al-Thabaiti, Royal Society of Chemistry, DOI:10.1039/c4nj01465k (2014) 1-12.
[19] S. Senthilkumaar, K. Rajendran, S. Banerjee, T.K. Chini, V. Sengodan, J. Mater. Sci.Semi cond. Process., **11**, (2008) 6.
[20] L.F.Koao, F.B.Dejene, H.C.Swart, J.R.Botha, J. Lumin., **143**, (2013) 463.
[21] V. Kumar, H.C. Swart, O.M. Ntwaeaborwa, R.E. Kroon, J.J. Terblans, S.K.K. Shaat A. Yousif and M.M. Duvenhage, Mat. Lett. **101**, (2013) 57.